Initial Atmospheric Corrosion of Zn: Influence of Humidity on the Adsorption of Formic Acid Studied by Vibrational Sum Frequency Spectroscopy

ARTICLE *in* THE JOURNAL OF PHYSICAL CHEMISTRY C · APRIL 2009

Impact Factor: 4.77 · DOI: 10.1021/jp900459q

3 AUTHORS, INCLUDING:

Jonas Hedberg
KTH Royal Institute of Technology
36 PUBLICATIONS **354** CITATIONS
SEE PROFILE

Christofer Leygraf
KTH Royal Institute of Technology
251 PUBLICATIONS **5,604** CITATIONS
SEE PROFILE

Initial Atmospheric Corrosion of Zn: Influence of Humidity on the Adsorption of Formic Acid Studied by Vibrational Sum Frequency Spectroscopy

Jonas Hedberg,*,† Steven Baldelli,‡ and Christofer Leygraf†

Division of Surface and Corrosion Science, Department of Chemistry, Royal Institute of Technology, SE-100 44 Stockholm, Sweden, and Department of Chemistry, University of Houston, Houston, Texas 77204-5003

Received: January 16, 2009

The ZnO/Zn surface exposed to formic acid undergoes a partial, reversible dissociation to formate ion, and a protonated surface oxide and is seen to have different hydration states depending on the relative humidity. Under high relative humidity conditions it exists as a formate coordinated to the surface with the oxygen atoms toward the surface and the C−H directed away into the vapor. In a dry environment a formic acid/formate intermediate is formed, although a substantial amount of dissociated species still are present, in both hydrated and nonhydrated form. The results may have implications on the initial atmospheric corrosion of Zn and emphasize that the ZnO/Zn surface is heterogeneous with a range of acid and basic sites for the adsorption of formate and the proton.

Introduction

The zinc/water/formic acid system studied is a model system to explore the fundamentals of indoor atmospheric corrosion of metals such as zinc, copper, and nickel, which is triggered by the presence of organic acids.[1] This paper has been preceded by an earlier study on the initial atmospheric corrosion of zinc induced by formic acid,[2] which presented parallel results from vibrational sum frequency spectroscopy (VSFS) and infrared reflection absorption spectroscopy (IRAS) allowing a comparison to be made between the nature of the monolayer of zinc formate formed at the zinc/water interface (VSFS) and in the multilayers, respectively (IRAS). The growth of the multilayer of zinc formate previously was shown to be humidity sensitive and governed by electrochemical reactions,[3] while the VSFS data indicated that the evolution of zinc formate is humidity independent, suggesting the initial formation of the zinc formate is not electrochemical in nature. The results further suggested that the zinc formates observed at the interface act as precursors for initial zinc dissolution, as discussed previously.[3,4]

The results also reveal molecular insight into the so-called memory effect of atmospheric corrosion, a phenomenon frequently observed on zinc, in which the initial periods of exposure of zinc have been shown to strongly influence the subsequent corrosion rate.[5,6] The most important factors responsible for this were seen to be rainfall and humidity conditions. Therefore, studies on the initial interaction involving water are of importance as it plays a role in the prolonged corrosion process.

In order to reveal further details regarding the initial formation of zinc formate interface species, this paper presents more details regarding the influence of water on the initial formation of zinc formate. In what follows results will be presented based on exposure of zinc to formic acid containing air that has been alternately humidified or dried, while following the chemical changes at the zinc/aqueous adlayer/air interfacial region with interface-sensitive VSFS.

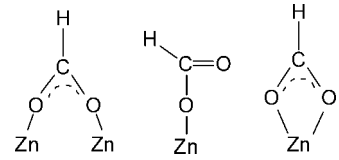

Figure 1. Three possible adsorption sites for formate on the ZnO/Zn surface (from left): bridging, monodentate, and bidentate configurations, respectively.

Formic acid, HCOOH, adsorbed onto a zinc oxide surface initially under goes an acid−base reaction in which the surface oxide is protonated and forms a surface hydroxyl group, Zn−OH.[7] The conjugate base of this reaction is the formate ion, $HCOO^-$, which remains on the surface. Formate is typically coordinated to Zn^{2+} sites in a bridging, monodentate, or bidentate configuration, as depicted in Figure 1.

Metal oxides in contact with water become hydroxylated to form a variety of surface OH species. These OH species have a range of acid−base properties depending on the coordination of the metal ion.[8−10] In general, the exposure of the metal oxide surface to a vapor pressure of water will contain a thin water film with a thickness on the order of nanometers. This is the medium in which the corrosion reactions proceed.[11,12]

This paper reports the results on the coadsorption of water and formic acid on the surface of the ZnO/Zn surface. VSFS was used to identify the adsorption of formic acid by changes in the C−H and CO stretching frequencies as a function of relative humidity (RH). The results indicate that the initial formate species depends on if formic acid is introduced in high or low RH conditions. Formic acid adsorbed under dry conditions protonated the surface oxide to create formate and surface OH. However, in the presence of water, both water and formic acid generate surface OH, creating a different surface state for the adsorbed formate ion. Upon removal of the H_2O, i.e., low RH, both formic acid and formate are observed. The conversion of formate to a formate/formic acid intermediate occurs alternatively as water is added or removed from the system.

* Corresponding author: fax, +46 8 208284; e-mail, jhed@kth.se.
† Royal Institute of Technology.
‡ University of Houston.

10.1021/jp900459q CCC: $40.75
Published on Web 03/24/2009

Background

VSFS spectroscopy is a second-order nonlinear technique which is sensitive to molecules at the interface where the centrosymmetry of the bulk media is broken. Since molecules in the bulk liquid state are considered to be in an environment which has inversion symmetry, VSFS signal is not generated in the bulk, but only from the interface. Hence, it is a surface specific technique. VSFS spectroscopy has been described thoroughly in the literature.[13−16]

Sum frequency spectroscopy involves overlapping two laser beams (one a frequency tunable IR beam and the other with a fixed visible light frequency) on the surface to induce a nonlinear polarization response ($P^{(2)}$) at the interface which generates a third beam with a frequency equal to the sum of the two incident beams. The intensity of the SFG signal, $I(\omega_{SF})$, is proportional to the square of the induced polarization, where E refers to the electric fields of the visible and IR incoming beams as indicated in eq 1, where

$$\chi^{(2)} = \sum \chi_R{}^{(2)} + \chi_{NR}{}^{(2)}$$

$\chi_R{}^{(2)}$ is the resonant nonlinear susceptibility that relates to the average molecular response of $P^{(2)}$ while $\chi_{NR}{}^{(2)}$ is mostly due to the substrate. The resonant nonlinear susceptibility is shown in eq 2, where A is the strength of the nth transition moment. The amplitude, A, has contributions from Raman polarizability and IR dipole transition; hence, VSFS is only allowed if the vibrational mode is both IR and Raman active.

$$I(\omega_{SF}) \propto |P^{(2)} = \chi^{(2)}{:}E_{Vis}E_{IR}|^2 \quad (1)$$

$$\chi_R{}^{(2)} = \frac{A}{\omega_{IR} - \omega_n + i\Gamma_n} \quad (2)$$

ω_{IR} and ω_n refer to the frequencies of the incoming IR and the normal mode, respectively, while Γ_n is the damping constant.

Experimental Section

Sample Preparation and Exposure. The polycrystalline zinc samples (Goodfellow, 99.99% purity) were polished with SiC grit paper, from 500 mesh in steps down to 4000 mesh, in water. Diamond paste with particle sizes 3 μm, 1 μm, and, finally, 0.25 μm was used as the final polishing steps, with ethanol used as lubricant. In order to remove residual diamond particles, each sample was sonicated in ethanol for 5 min between each step. After being polished, each sample was sonicated twice in pure ethanol, rinsed with pure water, dried with nitrogen gas, and placed into the sample cell. There it was kept in dry N_2(g), and a spectrum taken before exposure was collected. All water used was obtained from a Millipore RiOs-8 and Milli-Q PLUS purification system, filtered through a 0.2 μm Millipak filter. The resistivity was 18.2 MΩ·cm.

The system for generating the corrosive air involves mixing three different flowing gases:[17] dry, humid, and dry containing formic acid. The dry air was generated by a Zander KEA adsorption dryer and was also filtered with a Labclear filter. The formic acid was obtained from a permeation tube (Vici Metronics) calibrated so that the concentration of formic acid was 120 ppb at the flow rates of this experiment. These three flows were mixed so that the relative humidity could be controlled between 0 and 100% and the flow velocity was approximately 4 cm/s along the sample surface, assuming a laminar flow. This flow rate is equivalent to the air velocity of stagnant indoor conditions. The total flow rate was 1200 cm^3/min. The relative humidity was measured with a Hygroclip probe (Swema, Sweden) to an accuracy of ±1.5% RH. The exposures were conducted at controlled temperatures (19 ± 0.5 °C).

To study the influence of water on the sample, the ZnO/Zn was first exposed to formic acid in either dry or humid air after which the formic acid supply to the sample was stopped and a spectrum collected. Next the humidity was changed between 0 and 90% humidity alternatively with collection of a spectrum at each RH. These experiments were performed in a Teflon cell in which the corrosive air entered from the top and was split up so that it was not directly impinging onto the sample. This is a similar geometry previously used in in situ atmospheric corrosion experiments.[17] The experiments were repeated at least three times.

The VSFS setup has been described in detail in a previous publication.[18] In short, an Ekspla Nd:YAG picosecond laser with an output wavelength of 1064 nm, 24 ps long pulses, and a repetition rate of 20 Hz was used to pump an optical generator/optical parametric amplifier (OPG/OPA) from Laservision. In the OPG/OPA an infrared and a visible beam are generated. The output energy from the OPG/OPA in the CH region (2800−3000 cm^{-1}) was around 300 and 40 μJ for frequencies lower than 2000 cm^{-1}. The infrared beam was scanned with a speed of 1 cm^{-1}/s. The energies of the infrared and visible beams were measured and used for normalization of the generated sum frequency intensity. In the experiments in the CH region the IR beam was unfocused; the size was about 4 mm in diameter. The visible beam was 1.5 cm in diameter in order to avoid sample damage. For the experiments in the region below 2000 cm^{-1}, where the IR energy was considerably lower, the beam was softly focused 2 cm behind the sample with a +200 mm BaF_2 lens.

The linearity of the detector and sum frequency signal was checked by changing the intensity of the IR and visible beams independently, checking that the normalized sum frequency response was the same for different energies of the incoming beam.

The intensity, I_{SF}, of the VSFS spectra was fitted to a Lorentzian function with Origin software. To account for experimental scattering of the data, the instrumental weighting option was used in the error analysis.

Discussion on Studied Interfaces. In these experiments there exists a thin layer of liquid water on the ZnO/Zn surface, especially at high RH. The thickness of this layer is in the order of a few nanometers.[19] As VSFS is a surface-sensitive technique, there is a concern as to which interface the sum frequency generated beam originates from: the solid−liquid and/or the vapor−liquid interface. To establish if the air−water interface could contribute to the sum frequency signal, an experiment on an aqueous solution saturated with zinc formate dihydrate was conducted. The results showed that there were no peaks in the CH region in either ssp or ppp polarizations. The appearance of the spectrum is almost identical to the pure water spectrum, although with a slightly lower intensity. This allows the conclusion that from the air−water interface there is no significant contribution to the spectrum in the C−H or CO region and that the sum frequency signal originates from the solid−liquid interface. More details on this can be found in another publication.[2]

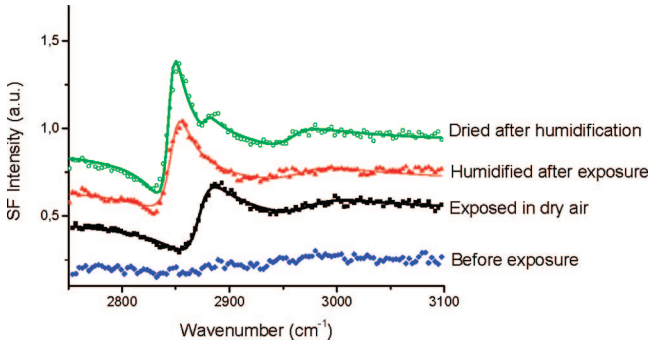

Figure 2. VSFS spectra in the CH region of ZnO/Zn: exposed to formic acid for 4 h in dry air (black squares), then humidified (red triangles), and, after that, dried again (green circles). The blue diamonds show the spectrum before exposure, in dry air. Solid lines are fitted curves to the data.

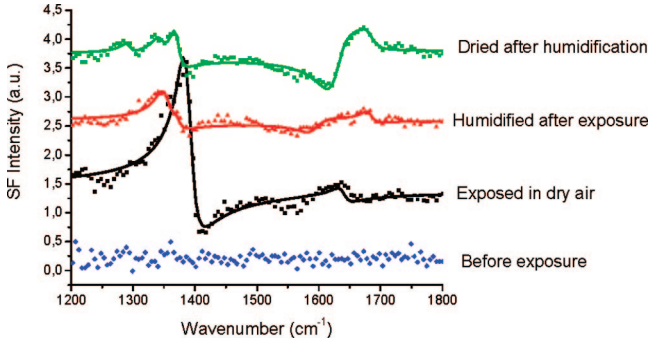

Figure 3. VSFS spectra in the CO region of ZnO/Zn: exposed to formic acid for 4 h in dry air (black squares), then humidified after exposure (red triangles), and dried again (green circles). The blue diamonds show the spectrum before exposure, in dry air. Solid lines are fitted curves to the data.

Results

Exposure of ZnO/Zn to Dry HCOOH. The VSFS spectra of the ZnO/Zn surface exposed to formic acid for the C−H and C═O stretching regions are presented in Figure 2 and Figure 3, respectively. The experiments proceed with the first exposure of formic acid in dry air, after that the formic acid supply was terminated, next the humidity was changed to 90%, and finally the sample was dried. The initial VSFS spectrum without exposure to formic acid is shown in Figure 2 in blue diamonds symbols; within the signal/noise ratio of the sum frequency signal there are no observable resonant features. Upon exposure to formic acid without water, one peak is observed at 2880 cm^{-1}, which is assigned to the C−H stretching vibration of formate ion, consistent with previous electron energy loss spectroscopy (EELS) and IR results,[20,21] where the C−H vibration is observed near 2900 cm^{-1} (limited by the resolution of the EELS spectrometer of ∼100 cm^{-1}). The infrared spectrum of solid sodium formate confirms the C−H vibration at 2870 cm^{-1}.[22]

The addition of water vapor to the system caused the peak to shift to 2850 cm^{-1}. This peak is also assigned to the C−H stretch of formate ion. The C−H band is sensitive to the hydration state of formate. The presence of water dramatically red shifts this peak approximately 40 cm^{-1}, to near 2830 cm^{-1}, as observed by both IR and Raman spectroscopy of bulk aqueous $HCOO^-Na^+$.[23,24] Thus the peak at 2850 cm^{-1} on the ZnO/Zn surface is attributed to the formate on the highly hydrated surface. Next, as the humidity in the system is removed, the spectrum appears with three peaks, one at 2850 cm^{-1}, one at 2880 cm^{-1}, and one at 2960 cm^{-1}. The latter peak could be due to the C−H of undissociated formic acid.[25−27] It could also originate from a monodentate configuration of formate on the surface.[28]

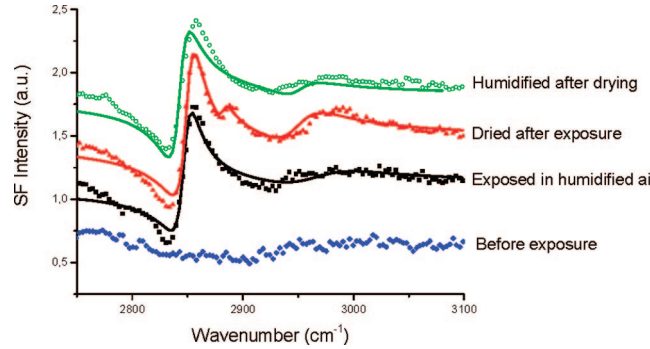

Figure 4. VSFS spectra in the CH region of ZnO/Zn: exposed to formic acid for 4 h in humid air (green), then dried (red), and, after that, humidified again (blue). Also shown is the spectrum before exposure, in humid air (black).

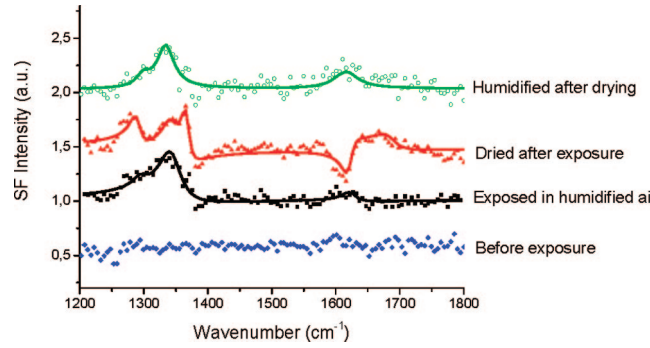

Figure 5. VSFS spectra in the CO region of Zn: exposed to formic acid after 4 h in humid air, exposed in humid (black), and dried after exposure (red). The solid lines are fitted curves to the data.

Additional evidence for the peak assignments is obtained by examination of the low-frequency carboxyl/carbonyl stretching region. The spectrum of formic acid exposed to the ZnO/Zn surface under dry conditions is shown in Figure 3. The spectra are presented in the same sequence of blank (ZnO/Zn), dry air and formic acid exposure, H_2O exposure with the formic acid exposure terminated, back to dry conditions, again without any formic acid present.

Under initial dosing of dry formic acid, a strong peak appears at 1385 cm^{-1} which is due to the symmetric carboxylate stretch, consistent with the previous works.[20−22,29] Next, the sample is exposed to water and a new peak appears at 1350 cm^{-1}, this peak is also due to the symmetric stretch of the carboxylate group of the hydrated formate.[30] Finally, removal of the water introduces several new peaks to the spectrum. Three peaks at 1280, 1340, and 1365 cm^{-1}, respectively, are observed. The latter two peaks are associated with carboxylate ion in hydrated environment, while the former has an ambiguous assignment. The C−O vibration from the C−OH group of formic acid could be responsible.[26] But the vibration could also, like in the case of the C−H peak at 2960 cm^{-1}, originate from a formate with a monodentate configuration.[28] The appearance of vibrations at 1620 and 1680 cm^{-1} again presents a problem in the assignment. The peaks could originate from either formic acid[31,32] or a formate ion. The reason that the peak at 1620 cm^{-1} appears as a dip is not completely understood. A dip is caused by a 180° change of phase of species adsorbed on metals and is interpreted in VSFS as a 180° change in orientation of the molecule.[33]

Exposure of ZnO/Zn to Humidified HCOOH. Next, the addition of formic acid in the presence of water changes the

TABLE 1: Vibrational assignment for the formate/formic acid, all values are in wavenumber (cm^{-1})

vibrational mode	this work	crystalline formic acid, IR, Raman [39]	crystalline formic acid, IR[26]	ZnO, IRAS [40]	ZnO(0001) HREELS[21]	ZnO(10$\bar{1}$0) HREELS[21]	ZnO powder, IR [41]	Zn formate powder, IR [42]
υ(CH)	2850	2960	2958	2860	2939	2895	2870	2911, 2900
	2880							
	2960							
$\upsilon_s(COO^-)$	1340			1345	1387	1363	1369	1355
	1365							
	1385							
$\upsilon_a(COO^-)$	1620[a]			1610	1610	1573	1572	1584
υ(C—O)	1280[a]	1270	1255,1224					
υ(C═O)	1620[a]	1605,1642	1703,1609					
	1680[a]							

[a] Tentative assignments.

initial state of the adsorbed formate ion. The VSFS spectra for these exposures are presented in Figure 4 and Figure 5, for the C—H and CO regions, respectively. In Figure 4 for exposure in humid air and formic acid, there is no 2880 cm^{-1} peak observed, only the 2850 cm^{-1} peak. However, as seen in the previous section, the 2880 cm^{-1} peak is present upon removing the water from the system, while the peak at 2850 cm^{-1} remains. Similarly, in Figure 5, the CO region shows the appearance of the 1340 cm^{-1} peak after exposure in humid air. There is also a weak peak at 1290 cm^{-1}. When dried there are additional peaks at 1280, 1365, 1620, and 1680 cm^{-1}. Humidification brings the spectrum back reversibly to the state as it was before being dried. Thus the reversible process of formate to formate/formic acid intermediate is observed as discussed in the previous section, except there is no initial formation of the 2880 and 1385 cm^{-1} peaks.

Discussion

The surface chemistry of zinc oxide is one of the most complicated of the oxides. The low Miller index surfaces ZnO(0001) and ZnO(000$\bar{1}$) are polar surfaces, were the latter is oxygen terminated and basic and the former is zinc terminated and acidic. The nonpolar surface ZnO(10$\bar{1}$0) is a mixture of acidic and basic sites. Therefore as the surface termination changes between the two polar surface terminations, the surface chemistry varies greatly.[9,34] Even "perfect" ZnO surfaces contain a large amount of defects.[35] Thus, on a polycrystalline surface, which is used in this work, the chemistry is widely varied and a multitude of adsorption configurations of formic acid onto the zinc oxide surface are expected.

It is well-known that exposure of metal oxides to water creates a surface terminated by hydroxyl groups that vary in their acid/base properties depending on the metal involved and its coordination.[9,35,36] Water vapor in contact with the ZnO surface produces Zn—OH groups. Similarly, ZnO in contact with HCOOH creates surface OH and formate species.[20,29,37]

$$ZnO + HCOOH \rightarrow Zn(OH)(OOCH)$$

The precise coordination of the formate ion to the zinc oxide surface is ambiguous, and any or all three structures in Figure 1 have been proposed.[20,21,29,37] VSFS data are consistent with the formate/formic acid coordinating to the surface through the carboxylate group, since similar vibrational frequencies are observed compared to the literature (see Table 1). Due to the amphoteric nature of the ZnO surface and the large variety of sites available on this polycrystalline surface, many configurations are possible as reflected in the range of assignments for formic acid on ZnO given in Table 1. Similarly, even bulk zinc formate has two different crystal structures with distinct vibrational spectra.[38]

Several observations are noted from the results of these experiments, which are combined to provide a physical view on the adsorption of water and formic acid on the ZnO/Zn surface.

1. The appearance of the C—H peak at 2880 cm^{-1} is linked to the symmetric COO^- peak at 1385 cm^{-1}.

2. The C—H peak at 2850 cm^{-1} is related to the COO^- peak at 1340 cm^{-1}.

3. The peak at 2960 cm^{-1} is related to the 1280, 1620, and 1680 cm^{-1} peaks.

Adsorption of Water and Formic Acid to the ZnO Surface. The formic acid that is introduced to a relatively dry surface will dissociate to create a surface formate and a surface hydroxyl group. This is observed as the peaks at 2880 and 1385 cm^{-1}, respectively. Under these conditions there is low humidity and the formate has only little water to interact with; therefore the dissociation is driven mostly by the protonation of the ZnO surface. This is contrasted by the situation with water present wheres the major species is formate ion but in a more hydrated environment so the peak is observed at 2850 cm^{-1}.[23] The presence of water has two potential roles in this process; solvation of the formate ion, and/or hydroxylation of the ZnO surface. Thus under humid conditions the spectra of Figure 1 are nearly identical to those in Figure 3. In addition the peak at 1385 cm^{-1} is formate under low humidity conditions,[20,21] which shifts to 1340 cm^{-1} upon addition of water to the system, consistent with the observations of formate ion in solution or hydrating environment.[24,30]

Removal of water results in a change in the VSFS spectra in both the CH and CO regions. The reappearance of the 2880 cm^{-1} and appearance of 1365 cm^{-1} peak suggest the formate species in a low hydration environment. However, the peaks at 2850 and 1340 cm^{-1} are present and indicate that this hydrated formate species is still adsorbed to the surface. An additional species is also seen when the water is removed in addition to the hydrated and less hydrated formate. As introduced earlier, the peaks at 1280, 1620, and 1680 cm^{-1} are associated with either physisorbed formic acid or formate with a mondentate configuration. However, the frequency of the peaks does not match either of the two configurations completely. Note for example that the frequencies of formic acid that matches the peaks in this work only have been observed at temperatures below 80 K[31,32] and also that the peak at 2960 cm^{-1} is slightly higher than that for a proposed monodentate configuration.[28] There are other studies which also point in different directions. A theoretical study indicated the monodentate is more favorable energetically over physisorbed formic acid for a zinc ion

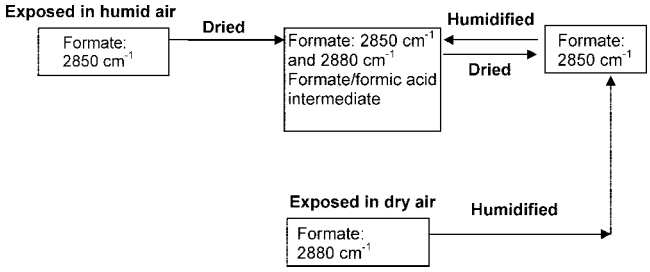

Figure 6. Summary of the changes in formate species upon removal and introduction of water on the surface of zinc exposed to formic acid in either humid or dry air, as deduced by VSFS.

interacting with water and formic acid.[43] But on the other hand, formic has been observed at room temperature for Zn(0001) exposed to formic acid, as is desorbed in TPD experiments at 370 K.[44] The conclusion is that an intermediate type of configuration is observed, which is possibly a mixture between monodentate and formic acid. It is not fully protonated formic acid and also not a pure monodentate type of formate.

The process of forming the formate/formic acid intermediate is then reversible as reintroduction of water vapor produces the hydrated surface species, as seen in the disappearance of the peaks at 1280, 1620, and 1680 cm^{-1}. The changes of the surface species when varying the humidity for zinc exposed to formic acid in dry or humid air are summarized in Figure 6.

The formation of undissociated formic acid with low RH is unexpected. The K_a for dissociation of formic acid is 1.7×10^{-4}, while the dissociation of $Zn(OH)_2 \rightarrow H^+ + Zn(O)(OH)^-$ is 1.2×10^{-17}, as an approximation to the surface species. It is more likely that the adsorbed formate ion is still interacting with the proton on the surface to help stabilize the adsorption. Theoretical studies indicate that the formic acid can dissociate on the surface creating a structure with one oxygen atom of the formate toward the surface OH.[37] This structure is possibly stabilized by water. It has been suggested from theoretical models[37] that the formate strongly interacts with the proton from the more acidic—zinc rich—sites, i.e., a $Zn-(OH)^+-Zn$ type structure, where the proton is at a bridging oxygen atom. Due to the amphoteric nature of the ZnO surface, it is expected that a range of acidic and basic sites exist. This leads to the formation of intermediate type of formate/formic acid at dry conditions and hydrate formate at humid conditions.

Conclusions

Formic acid on ZnO surface undergoes a partly reversible dissociation to formate ion. Under humid conditions it exists as a formate coordinated to the surface with the oxygen atoms toward the surface and the C−H oriented away from the bulk oxide. In dry environment a formate/formic acid intermediate configuration is seen although a substantial amount of dissociated species exists. The results emphasize that the ZnO surface is heterogeneous with a range of acid and basic sites. Water is important in the atmospheric corrosion of zinc induced by formic acid, seen in the sensitivity of the adsorption state of the formate on the zinc surface.

Acknowledgment. S. Baldelli would like to thank NSF (CHE-0650779) for funding. The Swedish Research Council (VR) is gratefully acknowledged for financial support.

References and Notes

(1) Persson, D.; Leygraf, C. *J. Electrochem. Soc.* **1995**, *142*, 1468.
(2) Hedberg, J.; Henriquez, J.; Baldelli, S.; Johnson, C. M.; Leygraf, C. *J. Phys. Chem. C* **2009**, *113*, 2088.
(3) Johnson, C. M.; Leygraf, C. *J. Electrochem. Soc.* **2006**, *153*, B542.
(4) Johnson, C. M.; Leygraf, C. *J. Electrochem. Soc.* **2006**, *153*, B547.
(5) Ellis, O. B. *ASTM Proc. Am. Soc. Testing Mater.* **1947**, 152.
(6) Guttman, H. In *Metal Corrosion in the Atmosphere*; ASTM special technical publication 435Dean, S. W., Jr , Rhea, E. C., Eds.; American Society for Testing and Materials: Philadelphia, PA, 1968; p 223
(7) Petrie, W. T.; Vohs, J. M. *Surf. Sci.* **1991**, *245*, 315.
(8) Brown, G. E.; Henrich, V. E.; Casey, W. H.; Clark, D. L.; Eggleston, C.; Felmy, A.; Goodman, D. W.; Gratzel, M.; Maciel, G.; McCarthy, M. I.; Nealson, K. H.; Sverjensky, D. A.; Toney, M. F.; Zachara, J. M. *Chem. Rev.* **1999**, *99*, 77.
(9) Henrich, V. E.; Cox, P. A. *The Surface Science of Metal Oxides*; Cambridge University Press: New York, 1994.
(10) Barteau, M. A. *Chem. Rev.* **1996**, *96*, 1413.
(11) Somorjai, G. A. *Introduction to Surface Chemistry and Catalysis*, 1st ed.; John Wiley and Sons, Inc.: New York, 1994.
(12) Leygraf, C.; Graedel, T. *Atmospheric Corrosion*; John Wiley and Sons: New York, 2000.
(13) Bain, C. D. *J. Chem. Soc., Faraday Trans.* **1995**, *91*, 1281.
(14) Miranda, P. B.; Shen, Y. R. *J. Phys. Chem. B* **1999**, *103*, 3292.
(15) Buck, M.; Himmelhaus, M. *J. Vac. Sci. Technol., A* **2001**, *19*, 2717.
(16) Shultz, M.; Baldelli, S.; Schnitzer, C.; Simonelli, D. *J. Phys. Chem. B* **2002**, *106*, 5313.
(17) Aastrup, T.; Leygraf, C. *J. Electrochem. Soc.* **1997**, *144*, 2986.
(18) Johnson, M.; Leygraf, C.; Tyrode, E.; Rutland, M.; Baldelli, S. *J. Phys. Chem. B.* **2005**, *109*, 329.
(19) Mikhailovsky, Y. N. *Theoretical and engineering principles of atmospheric corrosion of metals, Atmospheric Corrosion*; Wiley: New York, 1982; p 82.
(20) Sen, P.; Rao, C. N. R. *Surf. Sci.* **1986**, *172*, 269.
(21) Crook, S.; Dhariwal, H.; Thornton, G. *Surf. Sci.* **1997**, *382*, 19.
(22) Newman, R. *J. Chem. Phys.* **1952**, *20*, 1663.
(23) Bartholomew, R. J.; Irish, D. E. *Can. J. Chem.* **1993**, *71*, 1728.
(24) Ito, K.; Bernstein, H. J. *Can. J. Chem.* **1956**, *34*, 170.
(25) Hirose, C.; Ishida, H.; Iwatsu, K.; Watanabe, N.; Kubota, J.; Wada, A.; Domen, K. *J. Chem. Phys.* **1998**, *108*, 5948.
(26) Millikan, R. C.; Pitzer, K. S. *J. Am. Chem. Soc.* **1958**, *80*, 3515.
(27) Yokoyama, I.; Miwa, Y.; Machida, K. *J. Phys. Chem.* **1991**, *95*, 9740.
(28) Bandara, A.; Kubota, J.; Wada, A.; Domen, K.; Hirose, C. *J. Phys. Chem. B* **1997**, *101*, 361.
(29) Petrie, W. T.; Vohs, J. M. *Surf. Sci.* **1991**, *245*, 315.
(30) Spinner, E. *Aust. J. Chem.* **1985**, *38*, 47.
(31) Millikan, R. C. P.; Kenneth, S. *J. Am. Chem. Soc.* **1958**, *80*, 3515.
(32) Mikawa, Y.; Brasch, R. J. J. J.W. *J. Chem. Phys. Lett.* **1966**, *45*, 4751.
(33) Ward, R. N.; Duffy, D. C.; Davies, P. B.; Bain, C. D. *J. Phys. Chem.* **1994**, *98*, 8536.
(34) Akhter, S.; Lui, K.; Kung, H. H. *J. Phys. Chem.* **1985**, *89*, 1958.
(35) Dulub, O.; Diebold, U.; Kresse, G. *Phys. Rev. Lett.* **2003**, *90*, 016102.
(36) Meyer, B.; Marx, D.; Dulub, O.; Diebold, U.; Kunat, M.; Langenberg, D. *Angew. Chem., Int. Ed.* **2004**, *43*, 6642.
(37) Nakatsuji, H.; Yoshimoto, M.; Umemura, Y.; Takagi, S.; Hada, M. *J. Phys. Chem.* **1996**, *100*, 694.
(38) Viertellhaus, M.; Anson, C. E.; Powell, A. K. *Z. Anorg. Allg. Chem.* **2005**, *631*, 2365.
(39) Zelsmann, H. R.; Marechal, Y.; Chosson, A.; Faure, P. *J. Mol. Struct.* **1975**, *29*, 357.
(40) Johnson, C. M.; Leygraf, C. *J. Electrochem. Soc.* **2006**, *153*, B542.
(41) Ueno, A.; Onishi, T.; Tamaru, K. *Trans. Faraday Soc.* **1970**, *66*, 756.
(42) Baraldi, P. *Spectrochim. Acta* **1979**, *35A*, 1003.
(43) Tiraboschi, G.; Roques, B.-P.; Gresh, N. *J. Comput. Chem.* **1999**, *20*, 1379.
(44) Yoshihara, J.; Campbell, C. T. *Surf. Sci.* **1998**, *407*, 256.

JP900459Q